Fibre Diffraction Review 13, 38 - 42, 2005 doi: 10.1382/fdr.2005.1306

Flexible Filamentous Virus Structures from Fiber Diffraction

Gerald Stubbs, Lauren Parker, Justin Junn and Amy Kendall

Center for Structural Biology, Vanderbilt University, Nashville, TN 37232-8725, USA

Abstract

A combination of orientation using strong magnetic fields and the use of highly collimated synchrotron radiation has allowed the determination of the symmetry, surface structural features, and radial density distribution for potato virus X. A diffraction pattern from the related narcissus mosaic virus promises significantly more accurate determination of the radial density distribution. Diffraction patterns from the potyviruses wheat streak mosaic virus and bean common mosaic virus offer, for the first time, the possibility of similar determinations for potyviruses, economically the most important plant viruses in the world.

Filamentous plant viruses

Filamentous plant viruses have been the object of fiber diffraction studies since the 1930s. Bernal and Fankuchen (1941) published diffraction patterns from oriented sols of a number of viruses, including the rigid rod-shaped tobacco mosaic virus (TMV) and the flexible filamentous potato virus X (PVX).

TMV and related viruses (tobamoviruses) were studied extensively in the following years. The symmetry was determined from fiber diffraction patterns using an isomorphous mercury derivative (Franklin & Holmes, 1958), and found to be 49 subunits in three turns of the viral helix. The viruses were shown to be about 180 Å in diameter and to have a central hole of diameter 40 Å. A single strand of RNA follows the basic viral helix at a radius of about 40 Å (Caspar, 1956; Franklin, 1956a).

Isomorphous replacement was used by Barrett et al. (1972) to obtain an electron density map of TMV from fiber diffraction data at 10 Å resolution. The structure was determined at 4 Å resolution (Stubbs et al., 1977) using the technique of multi-dimensional isomorphous replacement (Stubbs & Diamond, 1975). This determination required six isomorphous heavy-atom derivatives. Further advances in data processing (Makowski, 1978), phasing (Stubbs & Makowski, 1982) and refinement (Stubbs et al., 1986) methods allowed the structure determination at 3.6 Å resolution (Namba & Stubbs, 1986), and eventually phase extension and refinement at 2.9 Å (Namba et al., 1989). The entire protein chain and the RNA were visible in the 2.9 Å map. Interpretation of the maps was aided by parallel studies by Klug's group on crystals of the isolated TMV coat protein, which led to an independent structure of a large part of the protein without RNA (Bloomer et al., 1978).

Other tobamoviruses had also interested the early workers; radial density distributions were determined for the U2 strain of TMV, cucumber virus 4, and the so-called "bean form" of the Nigerian cowpea strain of TMV, later called sunn-hemp mosaic virus (Franklin, 1956b; Holmes & Franklin, 1958). The structure of U2 was later determined by molecular replacement from TMV using fiber diffraction data at 3.5 Å resolution (Pattanayek & Stubbs, 1992), cucumber green mottle mosaic virus at 3.4 Å using a combination of isomorphous replacement and molecular replacement (Lobert & Stubbs, 1990; Wang & Stubbs, 1994), odontoglossum ringspot virus at 3.5 Å by molecular replacement (Planchart, 1995; Wang et al., 1998), and ribgrass mosaic virus (RMV) at 2.9 Å by molecular replacement (Wang et al., 1997). These four virus structures were all refined using the molecular dynamics refinement program F-XPLOR (Wang & Stubbs, 1993), so although the TMV data are probably the best tobamovirus fiber diffraction data available, the RMV structure is probably the best determined structure.

Despite the early work of Bernal and Fankuchen, many years were to elapse before significant progress could be made with fiber diffraction from the flexible filamentous potexviruses. Beginning in the 1960s, Tollin, Wilson, and their colleagues determined helical pitch values and symmetries for PVX, narcissus mosaic virus (NMV), white clover mosaic virus, papaya mosaic virus, and clover yellow mosaic virus (reviewed by Tollin and Wilson, 1985). These studies used diffraction from dried fibers of the viruses, supplemented by electron microscopic observations. Magnetically oriented sols (Yamashita et al., 1998) of potexviruses yielded dramatically improved diffraction patterns, however, and these patterns allowed Parker et al. (2002) to determine the symmetry of PVX with considerably more accuracy, and to construct a low-resolution model whose features included deep grooves running both longitudinally and azimuthally in the viral outer surface.

There have been very limited studies of the rigid tobraviruses (Finch, 1965; Tollin & Wilson, 1971) and hordeiviruses (Finch, 1965), largely confined to determinations of the helical repeat and partial symmetry determinations.

Potyviruses make up the largest and most economically important plant virus group, including almost a third of the known plant viruses and responsible for over half the viral crop damage in the world (Riechmann et al., 1992; López-Moya and García, 1999). Nevertheless, structural studies of these viruses have been extremely limited, and published reports are in fact confined to estimates of the helical pitch (about 33 Å) based on the observation of a single reflection in optical diffraction patterns from electron micrographs (Varma et al., 1968; McDonald and Bancroft, 1977).

Specimen preparation

Fiber diffraction specimens were either oriented sols or dried fibers.

Oriented sols were made by an extension of the method of Gregory and Holmes (1965). Soft centrifuged virus pellets were drawn into glass capillaries and moved back and forth by aspiration. Shearing forces produced some orientation, demonstrated by viewing under a polarizing microscope. Following the method of Yamashita et al. (1998), the capillaries were sealed and centrifuged, typically for two to three days at around 5000 g. The dilute region at the top of the capillary was removed, and the capillaries were re-sealed and exposed to the high magnetic field of an NMR magnet (Bruker, Germany), typically 18.8 T for several days or weeks.

Dried fibers were made by suspending 5 µl drops of 10 mg/ml virus solution in a 1 mm gap between the ends of a re-moulded paper clip. Drying was controlled by maintaining a constant relative humidity of 86% in equilibrium with a saturated solution of potassium chloride. In later experiments, copper wire was used in order to allow drying in the magnetic field.

Diffraction data

Preliminary diffraction data were collected using an R-AXIS IV image plate detector and a Rigaku RU200 rotating anode X-ray generator equipped with a 100 µm source. Synchrotron data were collected at the BioCAT beam line of the Advanced Photon Source synchrotron at Argonne National Laboratory. The beam had dimensions of 35 µm vertically and 60 µm horizontally at the detector, and because of the long focal length of the mirrors, was very close to this size at the specimen. Data were recorded using a CCD detector approximately 115 mm from the specimen; a low-angle data set was recorded for PVX using a specimen-detector distance of ~400 mm. The detector measured approximately 85 mm horizontally and 50 mm vertically, with a pixel size of 24 µm square. The X-ray wavelength was 1.03 Å.

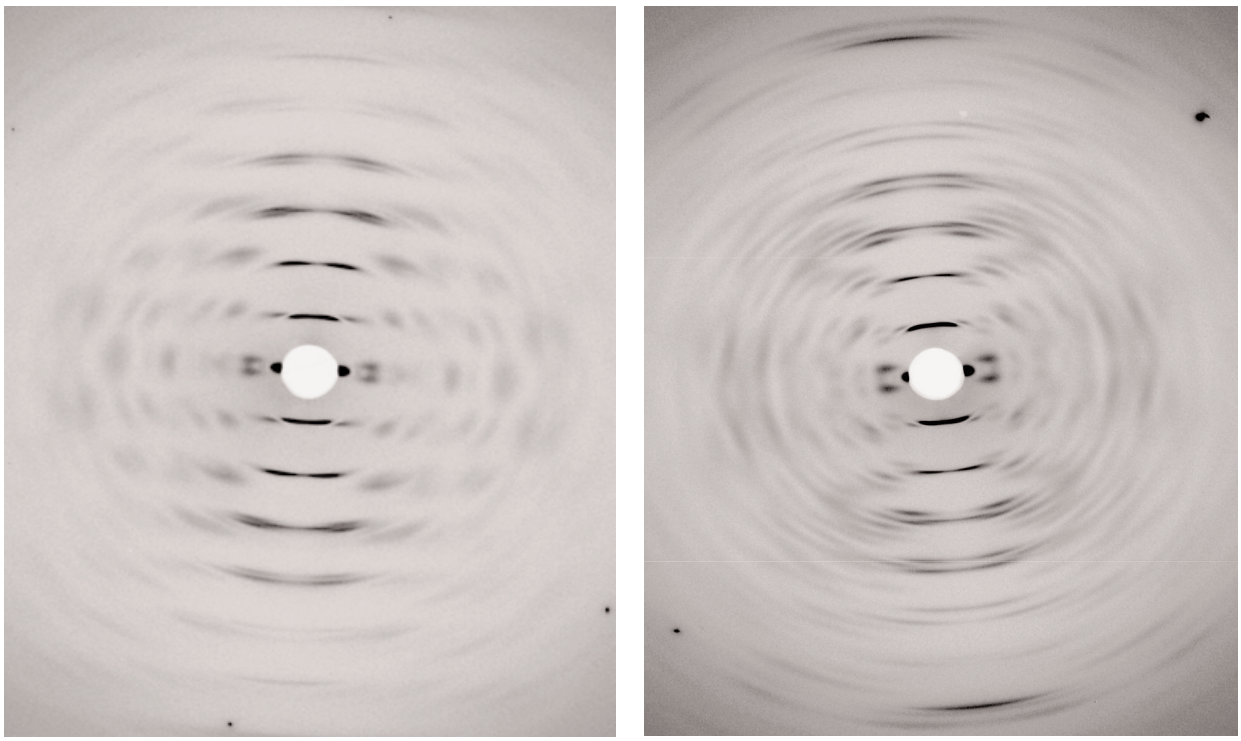

Figure 1: Diffraction patterns from magnetically oriented sols of potato virus X (left) and narcissus mosaic virus (right).

Data were analyzed using the public domain NIH Image program (developed at the U.S. National Institutes of Health, http://rsb.info.nih.gov/nih-image/) for direct measurements and the program WCEN (H. Wang and G. Stubbs, unpublished) for measurements in reciprocal space, including the fitting of layer lines.

Results

Figure 1 shows diffraction patterns from oriented sols of PVX and NMV.

The patterns exhibit, as expected from the similarity between the two viruses, very similar distributions of diffracted intensity. The strong intensities on the first layer lines and on the first near-meridional layer lines indicate the presence of deep intersecting sets of grooves running longitudinally and azimuthally in the viral surfaces (discussed for PVX by Parker et al., 2002). Both viruses exhibit a helical pitch of about 34.5 Å.

The most noteworthy difference between the two patterns is in the layer line spacing. In the PVX pattern, the first layer line is located at about one tenth of the distance of the first near-meridional layer line from the equator. Taken together with other data, this spacing suggests that there are 8.9 subunits per turn of the viral helix. In the NMV pattern, the first layer line is at one fifth of the near-meridional line spacing, indicating that there are only 8.8 subunits per turn. These values are similar to those obtained from lower resolution patterns by earlier workers (Tollin and Wilson, 1985).

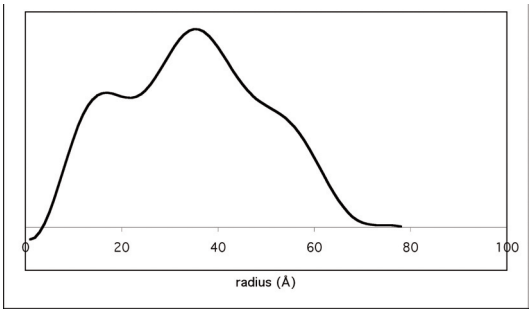

Figure 2: Radial density distribution calculated for PVX. Units on the ordinate are arbitrary

An approximate radial density distribution was determined for PVX. Equatorial structure factors were determined by integrating intensity in the z direction. Because of interference from the first layer line, data were obtainable only for three peaks, including the origin peak, which is behind the beamstop in Fig. 1 but was measured in the low-angle pattern. Structure factors at very low resolution (below 200 Å resolution, the inner part of the origin peak) were estimated as the transform of a cylinder, linearly scaled to be continuous with the measured part of the peak. The origin peak and the next peak were assigned phases of 0° and 180° by the maximum wavelength principle (Bragg and Perutz, 1952). Fourier-Bessel transforms were calculated assigning phases of both 0° and 180° to the third peak, but the resulting radial density distribution was only meaningful for the assigned phase of 180°. A phase of 0° produced a very large, physically implausible electron density peak at zero radius.

The radial density distribution is shown in Fig. 2. The distribution confirms the viral radius as about 65 Å, and shows that the radius of the hole in the center of the filament is about 10 Å, considerably smaller than the 20 Å hole in the tobamoviruses. One might speculate, by analogy with TMV (Caspar, 1956; Franklin, 1956) that the RNA lies at a radius of about 38 Å, corresponding to the highest peak in the density distribution.

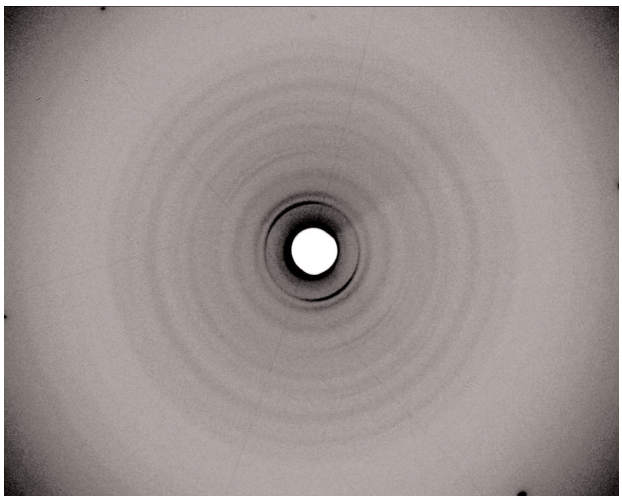

Figure 3: Diffraction pattern from a magnetically oriented sol of wheat streak mosaic virus.

Figure 3 shows a diffraction pattern from a magnetically oriented sol of WSMV. While the orientation does not approach that of potexvirus or tobamovirus specimens, there are numerous diffraction maxima, not previously observed in diffraction from any potyvirus. A series of sharp peaks can be interpreted as near-meridional maxima, corresponding to a helical pitch of 33.9 Å, and an off-meridional peak can be interpreted as a layer line at a spacing of 0.0856 Å-1. If this interpretation is correct, WSMV would have a helical symmetry of u + 0.9 subunits per turn, and comparison of the viral radius and coat protein molecular weight with those of TMV and PVX suggests that u = 6.

A preliminary diffraction pattern (not shown) has been obtained from a dried fiber of the potyvirus bean common mosaic virus (BCMV). This pattern was obtained using a laboratory X-ray source, and shows poor contrast. The orientation, however, is significantly better than that of the WSMV specimen, and it is possible to determine that the helical repeats for the two viruses are very similar.

Discussion

The fine collimation and high intensity of the X-ray beam at BioCAT allowed resolution of layer line 1 in the PVX pattern, and thus permitted accurate determination of the helical repeat and symmetry, a description of the surface features (Parker et al., 2002), and a preliminary determination of the radial density distribution. In the future, the greater layer line spacing in NMV should allow more accurate measurement of equatorial intensities, and a

more accurate radial density distribution. Application of both magnetic orientation and synchrotron radiation has allowed the first determination, albeit preliminary, of the symmetry and helical repeat distance for two potyviruses. Further work with the promising BCMV specimens should allow more accurate determination of these parameters, and offers excellent prospects for the elucidation of more structural features.

Acknowledgements

We thank Markus Voehler and the Vanderbilt University Biomolecular NMR facility for access to magnets, Tom Irving and his staff at BioCAT, David Baulcombe for the inoculum of potato virus X, David Robinson for the inoculum of narcissus mosaic virus, and Phil Berger and Pat Shiel for providing potyviruses. Virus structure research was supported by NSF grant MCB-0235653 and USDA grant 2003-01178. Fiber diffraction methods research was supported by NSF Research Coordination Network grant MCB-0234001. Use of the APS was supported by the U.S. Department of Energy under contract W-31-109-ENG-38. BioCAT is a NIH-supported Research Center RR-08630.

References

Barrett, A.N., Barrington Leigh, J., Holmes, K.C., Leberman, R., Mandelkow, E., von Sengbusch, P. and Klug, A. (1971) An electron-density map of tobacco mosaic virus at 10 Å resolution. Cold Spring Harbor Symp. Quant. Biol., 36, 433-448.

Bernal, J.D. and Fankuchen, I. (1941) X-ray and crystallographic studies of plant virus preparations. J. Gen. Physiol., 28, 111-165.

Bloomer, A.C., Champness, J.N., Bricogne, G., Staden, R. & Klug, A. (1978) Protein disk of tobacco mosaic virus at 2.8 Å resolution showing the interactions within and between subunits. Nature, 276, 362-368.

Bragg, W. L. and Perutz, M.V. (1952) The structure of haemoglobin, Proc. Roy. Soc. London, ser. A, 213, 425-435.

Caspar, D.L.D. (1956) Radial density distribution in the tobacco mosaic virus particle. Nature, 177, 928-928.

Finch, J.T. (1965) Preliminary X-ray diffraction studies on tobacco rattle and barley stripe mosaic viruses. J. Mol. Biol., 12, 612-619.

Franklin, R. E. (1956b) X-ray diffraction studies of cucumber virus 4 and three strains of tobacco mosaic virus. Biochim. Biophys. Acta, 19 203-211.

Franklin, R.E. (1956a) Location of the ribonucleic acid in the tobacco mosaic virus particle. Nature, 177, 928-930.

Franklin, R.E. and Holmes, K.C. (1958) Tobacco mosaic virus: application of the method of isomorphous replacement to the determination of the helical parameters and radial density distribution. Acta Cryst., 11, 213-220.

Gregory, J. and Holmes, K.C. (1965) Methods of preparing oriented tobacco mosaic virus sols for X-ray diffraction. J. Mol. Biol., 13, 796-801.

Holmes, K.C. and Franklin, R.E. (1958) The radial density distribution in some strains of tobacco mosaic virus. Virology, 6, 328-336.

Lobert, S. and Stubbs, G. (1990) Fiber diffraction analysis of cucumber green mottle mosaic virus using limited numbers of heavy-atom derivatives. Acta Cryst., A46, 993-997.

López-Moya, J.J. and García, J.A. (1999) Potyviruses (Potyviridae). In Encyclopedia of Virology 2nd edn., Vol. 3., Granoff, A. and Webster, R.G., eds. (Academic Press, London), 1369-1375.

Makowski, L. (1978) Processing of X-ray diffraction data from partially oriented specimens. J. Appl. Cryst., 11, 273-283.

McDonald, J.G. and Bancroft, J.B. (1977) Assembly studies on potato virus Y and its coat protein. J. Gen. Virol., 35, 251-263.

Namba, K. and Stubbs, G. (1986) Structure of tobacco mosaic virus at 3.6 Å resolution: implications for assembly. Science, 231, 1401-1406.

Namba, K., Pattanayek, R. and Stubbs, G. (1989) Visualization of protein-nucleic acid interactions in a virus: refinement of intact tobacco mosaic virus at 2.9 Å resolution by fiber diffraction data. J. Mol. Biol., 208, 307-325.

Parker, L., Kendall, A. and Stubbs, G. (2002) Surface features of potato virus X from fiber diffraction. Virology, 300, 291-295.

Pattanayek, R. and Stubbs, G. (1992) Structure of the U2 strain of tobacco mosaic virus refined at 3.5 Å resolution using x-ray fiber diffraction. J. Mol. Biol., 228, 516-528.

Planchart, A. (1995) X-ray fiber diffraction studies of odontoglossum ringspot virus. Ph.D. thesis, Vanderbilt University, Nashville.

Riechmann, J.L., Laín, S., and García, J.A. (1992) Highlights and prospects of potyvirus molecular biology. J. Gen. Virol., 73, 1-16.

Stubbs, G. and Diamond, R. (1975) The phase problem for cylindrically averaged diffraction patterns. Solution by isomorphous replacement and application to tobacco mosaic virus. Acta Cryst., A31, 709-718.

Stubbs, G. and Makowski, L. (1982). Coordinated use of isomorphous replacement and layer-line splitting in the phasing of fiber diffraction data. Acta Cryst., A38, 417-425.

Stubbs, G., Namba, K. and Makowski, L. (1986) Application of restrained least-squares refinement to fiber diffraction from macromolecular assemblies. Biophys. J., 49, 58-60.

Stubbs, G., Warren, S. and Holmes, K. (1977) Structure of RNA and RNA binding site in tobacco mosaic virus from a 4 Å map calculated from X-ray fibre diagrams. Nature, 267, 216-221.

Tollin, P. and Wilson, H.R. (1971) Some observations on the structure of the Campinas strain of tobacco rattle virus. J. Gen. Virol., 13, 433-440.

Tollin, P. and Wilson, H.R. (1985). Particle structure. In The Plant Viruses, Vol. 4: The Filamentous Plant Viruses, R.G. Milne, ed. (Plenum, New York), 51-83.

Varma, A., Gibbs, A.J., Woods, R.D. and Finch, J.T. (1968) Some observations on the structure of the filamentous particles of several plant viruses. J. Gen. Virol., 2, 107-114.

Wang, H. and Stubbs, G. (1993) Molecular dynamics in refinement against fiber diffraction data. Acta Cryst., A49, 504-513.

Wang, H. and Stubbs, G. (1994) Structure determination of cucumber green mottle mosaic virus by X-ray fiber diffraction. Significance for the evolution of tobamoviruses. J. Mol. Biol., 239, 371-384.

Wang, H., Culver, J.N. and Stubbs, G. (1997) Structure of ribgrass mosaic virus at 2.9 Å resolution: evolution and taxonomy of tobamoviruses. J. Mol. Biol., 269, 769-779.

Wang, H., Planchart, A. and Stubbs, G. (1998) Caspar carboxylates: the structural basis of tobamovirus disassembly, Biophys. J., 74, 633-638.

Yamashita, I., Suzuki, H. and Namba, K. (1998). Multiple-step method for making exceptionally well-oriented liquid-crystalline sols of macromolecular assemblies. J. Mol. Biol., 278, 609-615.